Modelling the biogenic CO2 exchange in urban and non-urban ecosystems through the assessment of light-response curve parameters

Article

Accepted Version

Creative Commons: Attribution-Noncommercial-No Derivative Works 4.0

It is advisable to refer to the publisher's version if you intend to cite from the work. See Guidance on citing.

the End User Agreement.

www.reading.ac.uk/centaur

CentAUR

Central Archive at the University of Reading

Reading's research outputs online

Abstract The biogenic CO$_2$ surface–atmosphere exchange is investigated and linked to vegetation cover fraction for seven sites (three urban and four non-urban) in the northern hemisphere. The non-rectangular hyperbola (NRH) is used to analyse the light-response curves during period of maximum ecophysiological processes, and to develop two models to simulate biogenic vertical CO$_2$ fluxes. First, a generalised set of NRH coefficients is calculated after linear regression analysis across urban and non-urban ecosystems. Second, site-specific NRH coefficients are calculated for a suburban area in Helsinki, Finland. The model includes a temperature driven equation to estimate ecosystem respiration, and variation of leaf area index to modulate emissions across the year. Eddy covariance measured CO$_2$ fluxes are used to evaluate the two models at the suburban Helsinki site and the generalised model also in Mediterranean ecosystem.

Both models can simulate the mean daily trend at monthly and seasonal scales. Modelled data typically fall within the range of variability of the observations (differences of the order of 10%). Additional information improves the models performance, notably the selection of the most vegetated wind direction in Helsinki. The general model performs reasonably well during daytime but it tends to underestimate CO$_2$ emissions at night. This reflects the model capability to catch photosynthesis processes occurring during the day, and the importance of the gross primary production (GPP) in modifying the net ecosystem exchange (NEE) of urban sites with different vegetation cover fraction. Therefore, the general model does not capture the differences in ecosystem respiration that skew nocturnal fluxes. The relation between the generalised NRH plateau parameter and vegetation cover improves (R^2 from 0.7 to 0.9) when only summer weekends with wind coming from the most vegetated sector in Helsinki and well-watered conditions for Mediterranean sites are included in the analysis.In the local model the inclusion of a temperature driven equation for estimating the ecosystem respiration instead of a constant value, does not improve the long-term simulations. In conclusion, both the general and local models have significant potential and offer valid modelling options of biogenic components of carbon exchange in urban and non-urban ecosystems.

Keywords: net ecosystem exchange (NEE); urban vegetation; photosynthesis; CO$_2$ emissions; eddy covariance; vegetation uptake

1 Introduction

Carbon dioxide is the most important anthropogenic greenhouse gas (GHG) in the atmosphere (IPCC, 2013). Over the past decade, CO$_2$ has been responsible for about 83% of the total increase of global radiative forcing (WMO, 2015). The global average atmospheric concentration in 2014 was 43% greater than its pre–industrial levels (Le Quéré et al., 2015). Anthropogenic activities, such as fossil fuel combustion, cement production, deforestation and replacement of natural or agricultural ecosystems by impervious surfaces (dwellings, roads, roofs etc.), are mainly responsible for this trend (Le Quéré et al., 2015). In recent years, more attention has been dedicated to study the role of cities in global climate change to consider mitigation strategies (Rozenzweig, 2010). Within their extent, cities emit 30–40% of total GHG emissions (Satterthwaite, 2008; Marcotullio et al., 2013; Marcotullio, 2016) and are responsible for 45–70% of total energy-related CO$_2$ emissions (IEA, 2008; Marcotullio et al., 2013; Marcotullio, 2016). With an estimated 66% of people living in urban areas by 2050 (UN, 2014), an increase in energy demand and carbon emissions is expected. Therefore, it is critical to deepen our understanding of the interaction between natural and anthropogenic processes in response to environmental conditions and urban morphology.

In contrast to natural ecosystems, CO$_2$ fluxes in cities derive from a complex balance between biogenic (ecosystem respiration, R$_{eco}$, and gross primary production, GPP) and human activity (i.e. traffic, household activities and heating systems in buildings, and human respiration). Analogous to vegetated ecosystems, the sum of R$_{eco}$ and GPP is the net ecosystem exchange (NEE). As the biogenic component (vegetation and soil) can behave differently in cities to natural ecosystems (Decina et al., 2016; Velasco et al., 2016), understanding the role of vegetation in sequestering the CO$_2$ emitted by anthropogenic sources has received a lot of attention within the scientific community recently. During the growing season, a negative correlation between CO$_2$ fluxes and vegetation cover fraction (λ_V) has been identified: as vegetation cover increases CO$_2$ emissions decrease because of the greater plant photosynthesis uptake (e.g., Velasco and Roth, 2010; Bergeron and Strachan, 2011; Ramamurthy and Pardyjak, 2011, Nordbo et al. 2012). Although plants help to reduce anthropogenic CO$_2$ emissions in cities, vegetation is unable to completely offset anthropogenic emissions, and urban annual carbon budgets are almost always positive both on a daily and seasonal scale (Moriwaki and Kanda, 2004; Velasco and Roth, 2010, Crawford et al., 2011). In cities where $\lambda_V \leq 34\%$, the role of lawns and trees in reducing net CO$_2$ emissions is increasingly less effective (Velasco and Roth, 2010; Bergeron and Strachan, 2011), and when λ_V is less than 5%, the biogenic contribution to the total carbon balance can be considered negligible (Moriwaki and Kanda, 2004; Matese et al., 2009; Velasco et al., 2009; Grimmond and Christen, 2012; Ward et al., 2015). Only parts of cities with $\lambda_V > 80\%$ may potentially be net annual sinks (Nordbo et al., 2012).

The micrometeorological Eddy Covariance (EC) technique has been applied to directly measure the local net energy and mass fluxes (e.g. NEE) in urban areas (Velasco and Roth, 2010; Grimmond and Christen, 2012). Empirical methods or models are needed to partition the measured urban net exchange into biogenic and anthropogenic components, as it is difficult to measure them separately. However, the estimation of carbon uptake by vegetation remains difficult due to the complexity of urban ecosystems and the variety of different species (Jo and McPherson, 1995; Velasco et al., 2013).

Light-response curves are often used to estimate the ecosystem respiration and carbon uptake as a function of photosynthetically active radiation (PAR) or solar radiation, and air temperature (Nemitz et al., 2002; Bergeron and Strachan, 2011; Christen et al., 2011; Crawford and Christen, 2015; Ward et al., 2015). Other methods (Weissert et al., 2014) used to partition EC measurements into its biogenic components are based on soil CO$_2$ efflux models (Velasco et al., 2013, 2016) and measurements (Christen et al., 2011; Järvi et al., 2012; Park et al., 2013), as well as leaf-level photosynthesis models (Soegaard and Møller–Jensen, 2003) and measurements (Christen et al., 2011; Peters and McFadden, 2012; Park et al., 2013; Björkegren and Grimmond, 2016). Estimates can also be based on similar non-urban vegetation types (Moriwaki and Kanda, 2004; Helfter et al., 2011), biomass allometric equations and growth rate predictive models (Nowak et al., 2008; Bjorkegren and Grimmond, 2016; Velasco et al., 2013, 2016),

and bottom-up approaches to estimate anthropogenic contributions (traffic, household activities, and human respiration) to subtract from the measured fluxes (Velasco et al., 2013, 2016).

The natural (vegetation plus bare soil) cover fraction has been used to estimate annual continental-scale urban NEE for North America, Europe and eastern Asia (Nordbo et al., 2012), but to our knowledge the relation between different urban and non-urban ecosystems, and their dependence on λ_V and environmental variables has not been investigated to reproduce the mean NEE daily trend.

The aim of this work is to develop two sets of model parameters that can be used in two different modelling approaches: a *general* (obtained after the comparison of light-response parameters across different sites) and a *local* (adjusted to site-specific light-response parameters) model. Both models estimate the CO$_2$ biogenic components of the urban carbon balance. The specific objectives are:

1. to investigate similarities in CO$_2$ vegetation uptake in urban and non-urban ecosystems;
2. to identify empirical relations among biogenic CO$_2$ flux, vegetation cover fraction, and environmental variables, in order to develop a *general* model which estimates the NEE biogenic components;
3. to test the *general* model both in suburban (Helsinki, Finland) and natural sites (Mediterranean maquis vegetation of Capo Caccia, Italy) to highlight how generalised light-response parameters adjust to different ecosystems and vegetation cover fractions, capturing the daily trend of biogenic CO$_2$ fluxes;
4. to compare the performances of the *general* model with those of the site-specific modelling approach.

CO$_2$ fluxes measured with the EC technique at seven different sites are analysed and linked to surface characteristics. The sites cover mid and high latitudes in the northern hemisphere, with different land uses and climates. For this reason, at each site the growing season period is only considered (summer for deciduous ecosystems except for one evergreen Mediterranean site for which the whole year is analysed). For Mediterranean climate the effect of soil water content is explored. After the development of two modelling approaches, the models are compared for the same period in a suburban neighbourhood in Helsinki. CO$_2$ flux observations of a natural Mediterranean site (Capo Caccia) are then used to verify the biogenic character of the *general* model.

2 Materials and methods

A brief description of the sites analysed to develop the models is given in Section 2.1. The choice of sites was driven by the relatively limited availability of long-term EC datasets in suburban ecosystems and the challenging task to partition EC measurements into its biogenic and anthropogenic components. Therefore, mostly biogenic vertical CO$_2$ fluxes spanning as wide range of vegetation covers (from natural to urban ecosystems), and accessible to the authors were considered. An initial assessment of light-response parameters focused on understanding their ability to explain the net CO$_2$ exchange differences across different urban-non-urban ecosystems. The relation between the estimated light-response coefficients and vegetation cover fraction could then be investigated to see how, and if, they were significantly related. Based on these preliminary results a *general* model is developed (Section 2.2). Another model (hereafter called *local*) is developed that uses light-response parameters estimated for an individual suburban site (Section 2.3). The two models are evaluated with independent data and statistical indices (Section 2.4).

2.1 Sites description and analysis

Seven sites with different vegetation types and cover fractions are used in this study: three Mediterranean vegetated sites (two vineyards and a maquis ecosystem), a North–American deciduous forest, and three suburban sites (Helsinki, Finland, Baltimore, USA, and Swindon, UK). The observed EC data are analysed for the three Mediterranean sites and Helsinki, whereas literature data are used for the other sites (Table 1).

Table 1: Eddy Covariance sites used in this study for the analysis of light-response curves and the development of the *general* and the *local* models. For three of them (*) data are derived from published figures.

Reference	Site	Latitude Longitude	Ecosystem type	Analysed period	Vegetation cover (λ_V)
Schmid et al. (2000)	Morgan–Monroe State Forest * (MMSF) (IN, USA)	39.32° N 86.42° W	Deciduous forest	5–9/1998	100%
Marras et al. (2011)	Capo Caccia (Alghero, Italy)	40.61° N 8.15° E	Mediterranean Maquis	1/2005–12/2010	~ 70%
Crawford et al. (2011)	Baltimore (MD, USA) *	39.41° N 76.52° W	Suburban	Summer (2002–2006)	67%
Järvi et al. (2012)	Helsinki (Finland)	60.20° N 24.97° E	Suburban	Summer weekends (2011–2012)	60% (veg. sector) 48% (all sectors)
Marras et al. (2015)	Serdiana (Italy)	39.36° N 9.12° E	Vineyard	Summer (2009–2011)	~ 50%
Marras (2008)	Montalcino (Italy)	43.08° N 11.80° E	Vineyard	Summer (2005–2006)	~ 50%
Ward et al. (2013)	Swindon (UK) *	51.58° N 1.80° W	Suburban	Summer (2011)	44%

The maximum vegetative cover of the two Italian vineyards (Serdiana in southern Sardinia, Marras et al., 2015; Montalcino in Tuscany, Marras et al., 2008) is about 50% during the summer growing season (remainder bare soil). The grapevines (mean height 2.0 m) have EC data collected at 2.8 m above the ground, in different summer periods. Precipitation occurs mainly in spring and late autumn. The Mediterranean maquis (schlerophyllous species) evergreen ecosystem of short shrubs, located in a natural reserve on the North–West Sardinia coast (Capo Caccia, Alghero, Italy, Marras et al., 2011), has a maximum canopy height of 2–

2.5 m and λ_V is 70% on average. Vegetation is naturally well watered during winter and early spring, but prolonged elevated temperatures and water stress conditions occur in summer. Eddy covariance measurements (height = 3.5 m) for five years are used in this study. At both Sardinian sites also soil water content (SWC) measurements at 0.20 m depth are collected. The Morgan–Monroe State Forest (MMSF), a managed mixed broadleaf deciduous forest located in South Central Indiana (USA), has complete vegetation cover in summer and a mean canopy height of 25–27 m. Annual EC data (March 1998–February 1999) observed at 46 m height tower (Schmid et al., 2000) are analysed.

A residential area (3 km north from the city centre) of Swindon (UK) with 44% vegetation cover (500 m radius) consisting of 80% grass (i.e. parks and gardens, λ_V = 36%) and 20% deciduous trees and shrubs (λ_V = 9%) with a mean height of 6 m (Ward et al., 2013), and with EC measurements at 12.5 m from May 2011 to April 2012, is analysed. In Baltimore (Maryland, USA), in the suburban area of Cub Hill, EC CO_2 fluxes monitored at 41.2 m for five years (2002–2006) are investigated. The highly vegetated area (67.4%) has mostly deciduous trees (mean height = 11.4 m, 80% of total vegetation, λ_V = 54%) and grass from parks and lawns (20% of total vegetation, λ_V = 14%) (Crawford et al., 2011).

In Helsinki (Finland), 4 km north–east of the city centre area, EC sensors are mounted 31 m above the ground of an area with highly variable fetch (see Vesala et al., 2008; Järvi et al., 2012, 2014 for more details). The analysis is split into three sectors based on the predominate land cover: roads (40°–180°), vegetation (180°–320°), and buildings (320°–40°). The vegetation (average height = 9 m) is composed of gardens, grass area, and deciduous trees (Vesala et al., 2008). Around the EC tower, λ_V is 48% (800 m radius) but it increases to 60% within the vegetated sector (800 m radius). EC data are available since late 2004 (Järvi et al., 2009).

For all sites, after generally accepted quality control of EC data (Webb et al., 1980; Baldocchi, 1997; Aubinet et al., 1999; Schmid et al., 2000; Papale et al., 2006), analysis of the growing season (i.e. summer for deciduous ecosystems) is undertaken. Note as the Mediterranean maquis site of Capo Caccia is evergreen the whole year is used.

The data from six sites (excluding Helsinki) are used to develop a *general* model; the EC measurements from Helsinki suburban site (summers 2011 and 2012) are used to develop a *local* model. Finally, data from Helsinki (summer 2010) are used to evaluate both models, and from Capo Caccia (January–March 2011) the *general* model.

2.2 General model development
To estimate the NEE biogenic components (i.e. NEE = R_{eco}+GPP) in urban and non-urban ecosystems, the analysis of the light-response curves is undertaken (Table 1, all sites except Helsinki). Given the wide range of equations available, many authors (Marshall and Biscoe, 1980; Boote and Loomis, 1991; Ögren, 1993; Gilmanov et al., 2003; Stoy et al., 2006; Lasslop et al., 2010) suggest that the non-rectangular hyperbola (NRH) (Rabinowitch, 1951) is a better fit to observed light-response curves than the rectangular hyperbola equation (Michaelis–Menten function, Ruimy et al., 1995). Hence, NRH is used in this study to describe the respiration processes and the photosynthetic response to PAR.

GPP is obtained as the lower root of the quadratic equation:

$$\theta GPP^2 - (\alpha PAR + \beta)GPP + \alpha\beta PAR = 0 \qquad (1)$$

where α (μmol CO_2 μmol photons^{-1}) is the mean apparent ecosystem quantum yield and represents the initial slope of the light-response curve, β (μmol CO_2 m^{-2} s^{-1}) is the light-saturated gross photosynthesis of the canopy (plateau parameter), and θ is the convexity of the curve at light saturation (adimensional bending parameter). This curvature parameter determines the shape of the equation, allowing a better fit of the NRH model to experimental light-response curves (Marshall and Biscoe, 1980; Boote and Loomis, 1991; Ögren, 1993; Gilmanov et al., 2003; Stoy et al., 2006; Lasslop et al., 2010). Introducing R_{eco} as an intercept parameter at zero light (γ, μmol CO_2 m^{-2} s^{-1}), and changing the sign of GPP in Eq. 1, the non-rectangular hyperbola equation is:

$$NEE = R_{eco} + GPP = \gamma - \frac{1}{2\theta}\{\alpha PAR + \beta - [(\alpha PAR + \beta)^2 - 4\alpha\beta\theta PAR]^{0.5}\} \qquad (2)$$

The α, β, γ and θ coefficients are estimated through non-linear least squares regression between measured net CO_2 exchange and Eq. 2. Daytime (global solar radiation, R_g > 5 W m^{-2}) median values of CO_2 flux measurements (in bins of 50 μmol m^{-2} s^{-1} of PAR classes) are used to analyse the experimental light-response curves. After the estimation of individual site coefficients, their dependence on λ_V is analysed. Simple linear regression is applied to investigate general trends of the NRH coefficients across the different ecosystems. The identified linear relations are used to build the *general* empirical biogenic model where the NRH coefficients are now expressed as a function of vegetation cover. In the *general* model PAR is inferred from R_g. Global solar radiation is converted into μmol m^{-2} s^{-1} using the median wavelength (0.55 μm) and assuming PAR is 0.46 of R_g (Tsubo and Walker, 2005). Therefore, the equation to estimate the biogenic CO_2 flux (F_{CO_2}) is:

$$F_{CO_2}(\lambda_V, R_g) = \gamma(\lambda_V) -$$
$$\frac{1}{2\theta} \cdot \{\alpha(\lambda_V) \cdot (0.46 \cdot R_g) + \beta(\lambda_V) - [(\alpha(\lambda_V) \cdot (0.46 \cdot R_g) + \beta(\lambda_V))^2 - 4 \cdot \alpha(\lambda_V) \cdot \beta(\lambda_V) \cdot \theta(\lambda_V) \cdot (0.46 \cdot R_g)]^{0.5}\} \quad (3)$$

Further investigation with the Serdiana vineyard and Capo Caccia Mediterranean maquis ecosystems are carried out to investigate the influence of soil water availability on the net CO_2 exchange. Observations are stratified and NRH coefficients (Eq. 2) estimated for each soil moisture class (not shown).

2.3 Local model development
A site-specific model is developed for Helsinki to assess the performance of an optimized *local* model relative to the *general* modelling approach (Section 2.2). Observations of summer weekend days (June–August 2011 and 2012) from the vegetated sector (180°–320°) are used to minimize the effect of anthropogenic CO_2 emissions.

As R_{eco} can be simulated as a function of air temperature (T_{air}), the γ parameter in Eq. 2 is replaced with the exponential equation:
$$R_{eco} = 3.23 \cdot e^{0.03 \cdot T_{air}} \tag{4}$$
using EC data (2008–2009) for the 200°–270° sector and comparing it with chamber measurements (Järvi et al., 2012). The narrower sector is used to minimize the influence from anthropogenic emissions. In this sector, there is a botanical garden with minor roads used primarily by cyclists and pedestrians. Through the use of a 50° moving window, to fit light-response curves, a sensitivity test is conducted across the whole vegetated sector (180°–320°). For each window, the NRH parameters (α, β and θ) are estimated using non-linear least squared regression (Eq. 2 with Eq. 4 replacing γ). Averaged values of the NRH coefficients are then calculated, for both the 180°–320° and 200°–270° sectors. The latter are used to develop the *local* model.

In the model the β coefficient and R_{eco} (Eq. 4) are scaled by the vegetation cover fraction corresponding to the 200°–270° wind sector ($\lambda_V = 61\%$), and multiplied by the λ_V of the actual sector considered. Moreover, as both β and R_{eco} correspond to summer, they need to be scaled to model other seasons (not shown in this study). This can be done based on the Leaf Area Index (LAI) calculated for deciduous trees using the SUEWS model (Järvi et al. 2011, 2014).

The final equation used in the *local* model to estimate F_{CO_2} is therefore:
$$F_{CO_2}(T_{air}, R_g, \lambda_V, LAI) = R_{eco}(T_{air}, LAI, \lambda_V) - $$
$$\frac{1}{2\theta} \cdot \left\{ \alpha \cdot (0.46 \cdot R_g) + \beta(LAI, \lambda_V) - \left[(\alpha \cdot (0.46 \cdot R_g) + \beta(LAI, \lambda_V))^2 - 4 \cdot \alpha \cdot \beta(LAI, \lambda_V) \cdot \theta \cdot (0.46 \cdot R_g) \right]^{0.5} \right\} \tag{5}$$

2.4 Models evaluation

Independent data are used to evaluate the models in Helsinki (*general*, Eq. 3, *local*, Eq. 5) and at the evergreen natural Mediterranean maquis site (Capo Caccia) (*general* only). The period when the growing season occurs, and least anthropogenic sources impact on the measured CO_2 fluxes differs. The summer months (June–August 2010) in Helsinki are evaluated with $\lambda_V = 48\%$ (all wind sectors) and $\lambda_V = 60\%$ (vegetation sector, 180°–320°). Data are stratified into workdays and weekends to evaluate the contribution of anthropogenic sources (i.e. vehicular traffic). For the unmanaged Capo Caccia site, all wind sectors are considered for non-drought and non-environmental stress conditions (January–March 2011).

The evaluation metrics used are: the coefficient of determination (R^2), the root mean square error (RMSE), the normalized root mean square error (nRMSE), the mean absolute error (MAE), the mean bias error (MBE), and the index of agreement (IOA).

3 Results

In this section, results of the general and local model development and testing are shown in Section 3.1 and Section 3.2, respectively.

3.1 General model

The NRH coefficients obtained at the six analysed sites from the fit of the light-response curves are given in Table 2.

Table 2: Coefficients (and standard errors) of the non-rectangular hyperbola (Eq. 2) estimated by non-linear least squares regression. All notations defined in text are significant with $P < 0.001$.

Site	λ_V [%]	γ [μmol CO_2 m^{-2} s^{-1}]	α [μmol CO_2 μmol photons^{-1}]	β [μmol CO_2 m^{-2} s^{-1}]	θ [dimensionless]
Morgan–Monroe State Forest	100	2.952 (0.426)	0.022 (0.001)	27.588 (1.584)	0.951 (0.028)
Capo Caccia	70	1.74 (0.229)	0.013 (0.001)	6.814 (0.285)	0.972 (0.018)
Baltimore	67	4.211 (0.412)	0.014 (0.001)	16.567 (0.938)	0.977 (0.019)
Serdiana	50	1.597 (0.355)	0.019 (0.003)	8.207 (0.486)	0.881 (0.063)
Montalcino	50	1.917 (0.241)	0.013 (0.001)	9.469 (0.475)	0.862 (0.058)
Swindon	44	4.473 (0.312)	0.009 (0.001)	8.106 (0.484)	0.980 (0.021)

The coefficients α and θ have little variability across the sites (0.013 μmol CO_2 μmol photons^{-1} and 0.118, respectively), compared to γ and β (2.88 μmol m^{-2} s^{-1} and 20.77 μmol m^{-2} s^{-1}, respectively). The highest γ values are related to the two suburban sites (4.21 μmol CO_2 m^{-2} s^{-1} for Baltimore, and 4.47 μmol m^{-2} s^{-1} for Swindon) where the anthropogenic contributions are most significant. Baltimore (67% of vegetation cover) also has high β value (16.57 μmol m^{-2} s^{-1}), with the Morgan–Monroe State Forest having the maximum (27.59 μmol m^{-2} s^{-1}, $\lambda_V = 100\%$). The α coefficient seems to relate to λ_V, with maximum values for the forest (0.022 μmol CO_2 μmol photons^{-1}) and minimum values in Swindon (0.009 μmol CO_2 μmol photons^{-1}). However, differences in vegetation type, CO_2 concentrations and environmental conditions affect this relation. To investigate the dependence of each coefficient on λ_V, the following relations are derived:
$$\begin{cases} \alpha = 0.005 + 0.016 \cdot \lambda_V; \ R^2 = 0.5 \\ \beta = -8.474 + 33.454 \cdot \lambda_V; \ R^2 = 0.7 \end{cases} \tag{6}$$

These are used in the *general* model (Eq. 3) to simulate the mean diurnal variability of the biogenic CO_2 flux. As the bending parameter θ, and the ecosystem respiration (γ), have no similar relation they are fixed to their median values (0.96 and 2.43 μmol m^{-2} s^{-1}, respectively).

To evaluate the *general* model two independent sites (Helsinki and Capo Caccia) are used. The Helsinki suburban area (Fig. 1, Table 3) has general agreement, with better model performance for the vegetated sector (180°–320°) especially during weekends (individual months $0.89 \leq R^2 \leq 0.97$; whole summer RMSE = 1.62 μmol m^{-2} s^{-1}, nRMSE = 0.12, MAE = 1.41 μmol m^{-2} s^{-1}).

Table 3: Evaluation metrics for the *general* model application in suburban Helsinki (all wind directions ($\lambda_V = 48\%$) and vegetation wind direction only ($\lambda_V = 60\%$)) and natural Capo Caccia. Metrics are: root mean squared error (RMSE, μmol CO$_2$ m^{-2} s^{-1}), normalized root mean squared error (nRMSE, dimensionless), mean absolute error (MAE, μmol CO$_2$ m^{-2} s^{-1}), mean bias error (MBE, μmol CO$_2$ m^{-2} s^{-1}), index of agreement (IOA, dimensionless), and coefficient of determination (R^2, dimensionless). Values are significant with $P < 0.001$

| Helsinki		All wind direction ($\lambda_V = 48\%$)						Vegetated wind direction ($\lambda_V = 60\%$)					
	Period	RMSE	nRMSE	MAE	MBE	IOA	R^2	RMSE	nRMSE	MAE	MBE	IOA	R^2
All days	**June**	2.81	0.23	2.57	-2.15	0.84	0.82	1.77	0.12	1.62	-0.61	0.97	0.95
	July	3.12	0.36	2.99	-2.99	0.79	0.91	2.22	0.18	1.98	-1.98	0.95	0.96
	August	6.04	0.92	5.29	-5.29	0.31	0.01	2.45	0.23	2.30	-2.30	0.91	0.95
	JJA	3.77	0.48	3.53	-3.53	0.67	0.77	1.90	0.15	1.65	-1.61	0.96	0.96
Workdays	**June**	4.09	0.33	3.65	-3.51	0.68	0.60	1.95	0.13	1.70	-0.87	0.96	0.90
	July	3.90	0.47	3.75	-3.75	0.71	0.87	2.54	0.19	2.27	-2.27	0.93	0.95
	August	7.72	0.89	6.55	-6.55	0.27	0.13	3.10	0.27	2.82	-2.82	0.86	0.89
	JJA	5.09	0.66	4.66	-4.66	0.50	0.46	2.34	0.19	2.02	-2.01	0.93	0.94
Weekend	**June**	3.20	0.20	2.75	0.85	0.86	0.95	2.02	0.13	1.80	-0.43	0.96	0.97
	July	1.92	0.16	1.63	-1.33	0.92	0.89	1.97	0.14	1.69	-1.55	0.96	0.93
	August	2.87	0.37	2.53	-2.53	0.73	0.72	2.09	0.17	1.89	-1.63	0.94	0.90
	JJA	1.73	0.16	1.56	-1.10	0.93	0.95	1.62	0.12	1.41	-1.10	0.97	0.97
Capo Caccia	**All wind direction ($\lambda_V = 70\%$)**												
All days	**January**	1.14	0.11	0.88	0.78	0.97	0.95						
	February	0.92	0.06	0.70	-0.01	0.99	0.97						
	March	1.20	0.08	0.93	0.21	0.99	0.95						
	JFM	0.63	0.05	0.53	0.23	0.99	0.98						
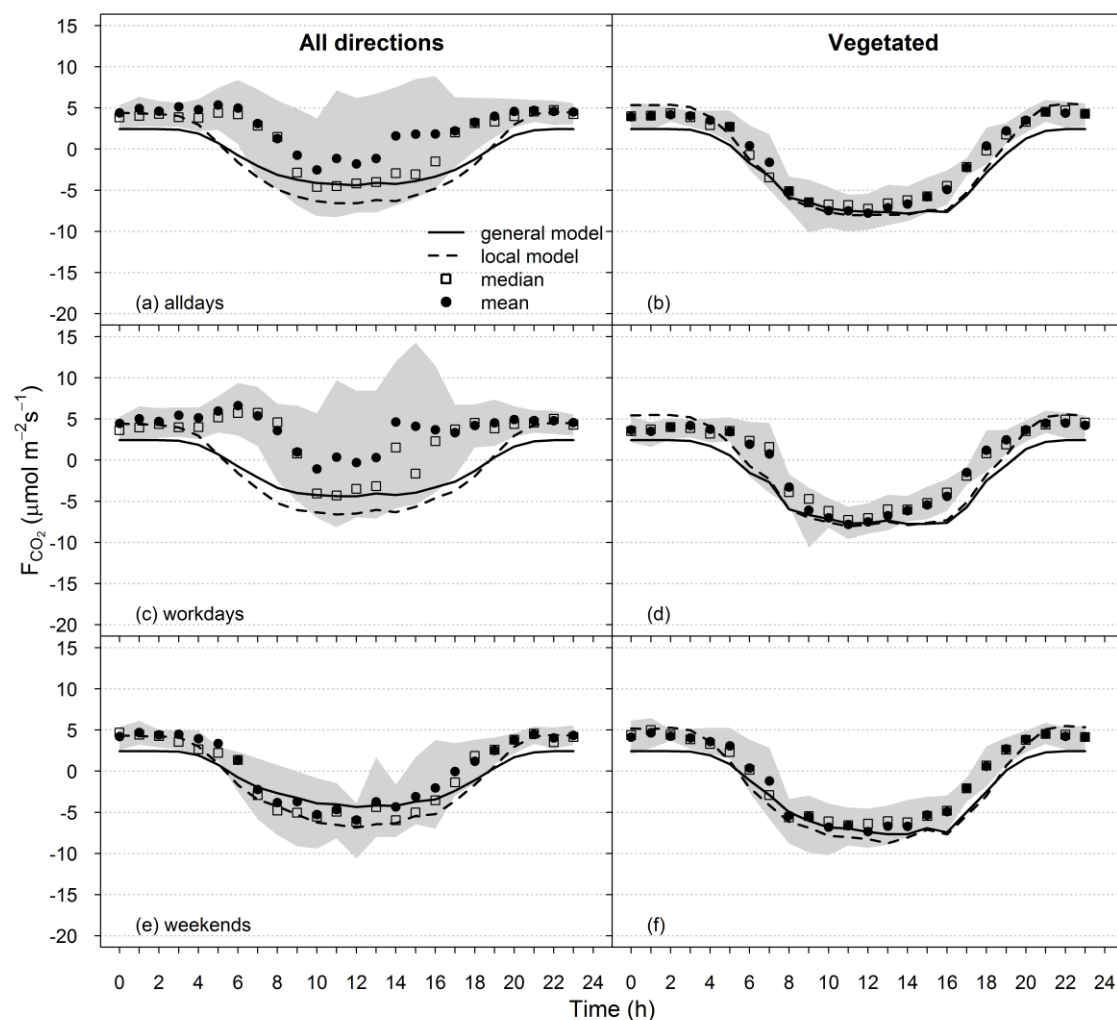
Fig. 1: Observed (markers, shading interquartile range hourly means) and modelled (general, solid, and local, dashed lines) mean CO$_2$ fluxes for Helsinki (June–August 2010) by wind direction (columns): (a, c, e) all sectors ($\lambda_V = 48\%$), and (b, d, f) vegetation sector only (see text) ($\lambda_V = 60\%$); stratified by days of week (rows) (a, b) all days, (c, d) workdays, and (e, f) weekends.

The mean daily trend of CO$_2$ fluxes is reproduced during the day and at night, but the *general* model slightly underestimates the measurements (-6.55 μmol m^{-2} s^{-1} $\leq$ MBE $\leq$ -0.43 μmol m^{-2} s^{-1}). However, as the model (unlike EC measurements) mainly neglects anthropogenic sources, the diurnal pattern is dominated by the daytime when the biogenic processes prevail. Therefore, it is unsurprising that greater discrepancies occur at night. Considering all wind directions (Fig. 1a, c, e), the traffic emissions from a major arterial route to the east of the EC tower remain a likely factor at night. In summer, there is an average of 1712 vehicles h^{-1} per day (June 1823, July 1516, August 1797 vehicles h^{-1}) with peaks associated with rush hour traffic (Fig. 1a, c), at around 07:00 (7.50 μmol m^{-2} s^{-1}) and 14:00 (8.87 μmol m^{-2} s^{-1}), and nighttime (22:00–06:00, 2.60 μmol m^{-2} s^{-1} on average). These include emissions from both local traffic and respiration (human, soil). The vegetated sector is the least impacted by rush hour traffic, with

smaller IQR (interquartile range), and very similar median and mean CO$_2$ fluxes. The model also fits the early morning and late evening periods. The maximum diurnal uptake is simulated well (all and vegetated sectors) with the model following the observed daytime median values. All simulations typically fall within the range of variability of the measured CO$_2$ fluxes (Fig. 1).

The second *general* model assessment uses data from a natural ecosystem (Capo Caccia) with no anthropogenic sources.
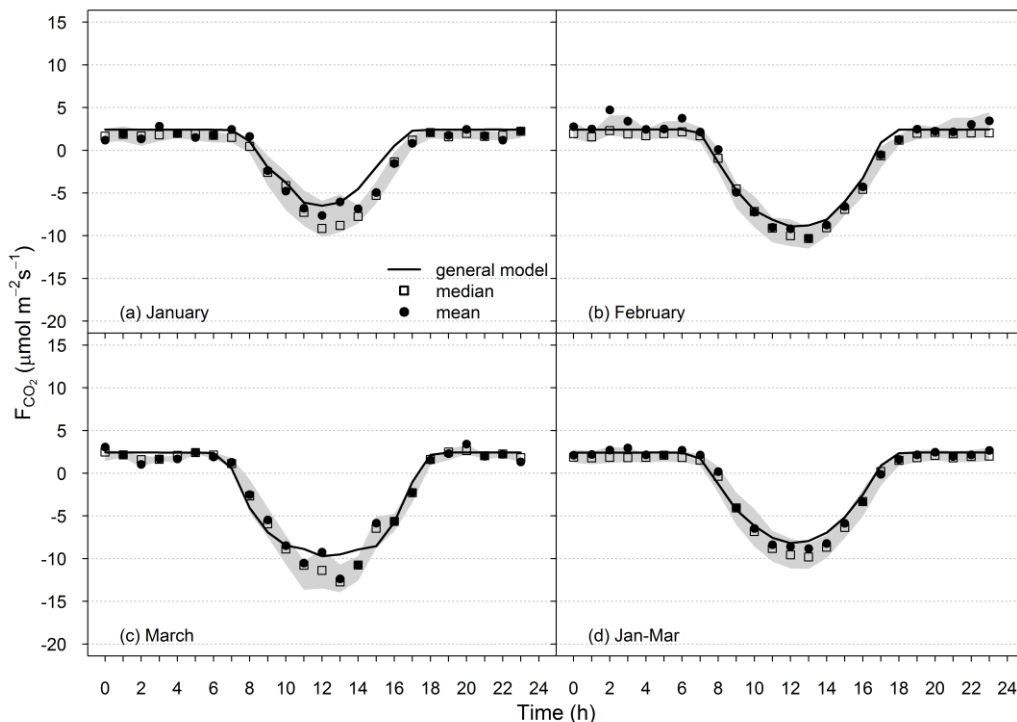
Here, the model has better performance with a smaller nRMSE (Table 3) than for Helsinki for both separate months and the period January–March ($0.05 \leq$ nRMSE ≤ 0.11). The mean daily trend of CO$_2$ fluxes is reproduced including the photosynthetic activity during the day and the ecosystem respiration processes at night (Fig. 2). For both sites, all periods analysed have statistical significance at 0.001 probability level for the linear regression metrics (Table 3).

Fig. 2: Observations (markers, shading IQR hourly means) and modelled (general, solid line) mean CO$_2$ fluxes for Capo Caccia for all wind directions ($\lambda_V = 0.70$): (a–c) individual months, and (d) the average for three months.

3.2 Local model

The sensitivity test undertaken in the Helsinki site vegetated sector (180°–320°) has interesting results (Table 4). The NRH coefficients α and θ have little variability (0.013 μmol CO$_2$ μmol photons^{-1} and 0.266, respectively) across the wind directions, compared to the β range (2.95 μmol CO$_2$ m^{-2} s^{-1}) which is on average 17.12 μmol CO$_2$ m^{-2} s^{-1} (Table 4).

This sector, with 60% vegetation, is similar to the botanical garden area (200°–270°). Thus, the averaged values for the 200°–270° wind sector (α = 0.031 μmol CO$_2$ μmol photons^{-1}, β = 17.793 μmol m^{-2} s^{-1}, θ = 0.723) are used in the final *local* model (Eq. 5), which is evaluated with the *general* model (Section 3.1) using 2010 Helsinki summer data. Results have good agreement with the EC measured CO$_2$ fluxes (Fig. 1, Table 5).

As for the *general* model, the simulations reproduce the mean daily trend of biogenic contributions, with best performance during weekends in the vegetated sector when the anthropogenic effects are smallest (R^2 = 0.97, IOA = 0.99, RMSE = 1.07 μmol m^{-2} s^{-1}, nRMSE = 0.08, MAE = 0.85 μmol m^{-2} s^{-1}) (Fig. 1f). As measurements include all components (biogenic and anthropogenic) but the model only accounts for vegetation uptake and ecosystem respiration, the negative MBE values (-0.13 μmol m^{-2} s^{-1} $\leq$ MBE $\leq$ -6.59 μmol m^{-2} s^{-1}) are not unexpected. This is confirmed if workdays are analysed (Fig. 1c, d) (1.75 μmol m^{-2} s^{-1} $\leq$ RMSE $\leq$ 8.78 μmol m^{-2} s^{-1}, 0.12 $\leq$ nRMSE $\leq$ 1.01, 1.43 μmol m^{-2} s^{-1} $\leq$ MAE $\leq$ 6.76 μmol m^{-2} s^{-1}). Better performance is obtained for weekends (all and vegetated sectors) (Fig. 1e, f) (1.07 μmol m^{-2} s^{-1} $\leq$ RMSE $\leq$ 3.43 μmol m^{-2} s^{-1}, 0.08 $\leq$ nRMSE $\leq$ 0.44, 0.85 μmol m^{-2} s^{-1} $\leq$ MAE $\leq$ 2.58 μmol m^{-2} s^{-1}). The diurnal trend is reproduced for all cases, with the mean modelled data typically within the hourly IQR of the observations (Fig. 1).

Table 4: Helsinki site non-rectangular hyperbola (Eq. 2) (a) coefficients (and standard errors) (b) mean (and standard deviations). All estimates (except those indicated *) are significant with P < 0.001 probability level. γ is estimated with Eq. 4. Land cover percentages for vegetation (λ_v), building (λ_b) and impervious (λ_i) within 800 m. Vegetated sector with a botanical garden in bold.

Sector (°)	λ_{v800}	λ_{b800}	λ_{i800}	α [μmol CO$_2$ μmol photons^{-1}]	β [μmol CO$_2$ m^{-2} s^{-1}]	θ [dimensionless]
a) 180–230	49	14	36	0.033 (0.005)	16.517 (0.827)	0.883 (0.091)
190–240	54	12	34	0.034 (0.005)	18.110 (1.269)	0.700 (0.187)
200–250	**59**	**10**	**31**	**0.031 (0.004)**	**17.746 (1.100)**	**0.762 (0.135)**
210–260	**63**	**9**	**27**	**0.031 (0.004)**	**17.757 (1.248)**	**0.705 (0.167)**
220–270	**65**	**10**	**25**	**0.030 (0.003)**	**17.876 (1.330)**	**0.702 (0.165)**
230–280	65	10	24	0.033 (0.005)	21.314 (3.362)*	0.378 (0.452)*
240–290	64	12	24	0.028 (0.003)	15.156 (0.996)	0.966 (0.046)
250–300	64	12	24	0.033 (0.004)	15.664 (0.980)	0.948 (0.066)
260–310	64	12	24	0.041 (0.009)	18.023 (2.217)	0.655 (0.338)*
270–320	66	10	24	0.033 (0.006)	17.206 (1.936)	0.951 (0.105)
b) Mean 180–320	60	11	28	0.033 (0.003)	17.117 (1.091)	0.827 (0.121)
Mean 200–270	**61**	**11**	**28**	**0.031 (0.000)**	**17.793 (0.072)**	**0.723 (0.034)**

Table 5: Evaluation metrics for the *local* model at the suburban Helsinki area (all wind directions (λv = 48%) and vegetation wind direction only (λv = 60%)). See Table 3 for other details.

Helsinki		All wind direction (λ_V = 48%)						Vegetated wind direction (λ_V = 60%)					
	Period	RMSE	nRMSE	MAE	MBE	IOA	R^2	RMSE	nRMSE	MAE	MBE	IOA	R^2
All days	**June**	3.58	0.29	3.02	-2.98	0.84	0.80	1.22	0.08	0.94	-0.22	0.99	0.95
	July	3.41	0.39	2.9	-2.73	0.83	0.89	1.79	0.14	1.57	-0.33	0.97	0.94
	August	6.99	1.07	5.43	-5.25	0.27	0.00	2.08	0.20	1.89	-0.79	0.95	0.93
	JJA	4.48	0.57	3.68	-3.64	0.68	0.75	1.44	0.12	1.22	-0.47	0.98	0.96
Workdays	**June**	5.31	0.44	4.4	-4.4	0.65	0.54	1.75	0.12	1.43	-0.36	0.97	0.9
	July	3.93	0.48	3.29	-3.22	0.78	0.86	1.88	0.14	1.61	-0.57	0.97	0.93
	August	8.78	1.01	6.76	-6.59	0.2	0.18	2.71	0.24	2.41	-1.3	0.92	0.85
	JJA	5.82	0.78	4.74	-4.72	0.5	0.48	1.89	0.15	1.6	-0.74	0.97	0.92
Weekend	**June**	1.94	0.13	1.56	-0.12	0.96	0.92	1.14	0.07	0.83	-0.19	0.99	0.97
	July	2.37	0.19	2.09	-1.44	0.92	0.85	1.93	0.13	1.62	0.03	0.97	0.93
	August	3.43	0.44	2.58	-2.29	0.76	0.72	1.83	0.15	1.6	-0.13	0.96	0.93
	JJA	1.77	0.17	1.35	-1.23	0.95	0.92	1.07	0.08	0.85	-0.14	0.99	0.97

4 Discussion

The three summer months (June–August 2010) used to evaluate both models in Helsinki had an average temperature of 18.4°C. Despite the 48% vegetation cover, anthropogenic CO$_2$ emissions are not offset in the area surrounding the EC tower. This area is a net CO$_2$ source (emitting 2.85 µmol m^{-2} s^{-1} on average) with lower (higher) values than average in June (August). Only the vegetated sector (180°–320°) is a net sink (average net CO$_2$ flux, -0.54 µmol m^{-2} s^{-1}) with enhanced uptake during the weekends: as a consequence of the decrease in anthropogenic activities the effect of vegetation uptake is more evident from daily trends, resulting in a more negative net CO$_2$ exchange (mean = -1.31 µmol m^{-2} s^{-1}).

The good performance of both models at both sites (differences of the order of 10%) suggests the proposed models are suitable for suburban neighbourhoods usually characterized by having a greater percentage of vegetation than city centres (e.g. > 40%) . The non-rectangular hyperbola allows an ecophysiological interpretation of its coefficients, that are affected by temperature and CO$_2$ concentration (Boote and Loomis, 1991). As noted earlier, this equation is often used to partition the net ecosystem exchange into GPP and R$_{eco}$, and calculate annual carbon budgets both in vegetated ecosystems (from evergreen or deciduous broadleaf forests, to grasslands, crops, prairie, pasture and savannas) (Gilmanov et al., 2003; Stoy et al., 2006; Lasslop et al., 2010), and in suburban sites (Nemitz et al., 2002; Bergeron and Strachan, 2011; Christen et al., 2011; Crawford and Christen, 2014).

Higher values of α indicates higher productivity. The Morgan–Monroe State Forest (0.022 µmol CO$_2$ µmol photons^{-1}) value is comparable to the growing season average at the Shidler tallgrass prairie (0.0195 µmol CO$_2$ µmol photons^{-1}) (Gilmanov et al., 2003). Moreover, the expectation of a constant mean ecosystem quantum efficiency is met with α having little variability across the sites and the 50° moving windows in Helsinki (0.013 µmol CO$_2$ µmol photons^{-1}, Table 2, 4). The bending parameter θ, does not drop below 0.70 and its range (0.70–0.98, Table 2, 4) is in accordance with those indicated by Marshall and Biscoe (1980), Boote and Loomis (1991), Ögren (1993) and Gilmanov et al. (2003).

The plateau parameter (β), representing the range between the ecosystem respiration and the maximum uptake, is a function of temperature, CO$_2$ concentration, vapor pressure deficit and light. It varies from about 7 µmol m^{-2} s^{-1} in the Mediterranean maquis ecosystem to about 28 µmol m^{-2} s^{-1} at the Morgan–Monroe State Forest (Table 2), and is on average about 18 µmol m^{-2} s^{-1} within the Helsinki most vegetated sector during the summer weekends (Table 4).

4.1 Importance of soil water availability

Investigation into the dependence of the six site-specific NRH coefficients (Table 2) on vegetation cover highlights a general increase of β values with λ_V (Eq. 6) (R^2 = 0.74). However, in semi-arid ecosystems, such as the Sardinian (Mediterranean) sites, soil water content plays an important role that should not be neglected as vegetation may encounter stress conditions that alter ecophysiological processes (Huxman et al., 2004).
In both the Serdiana vineyard and Capo Caccia maquis ecosystems, the SWC variability is limited. In the vineyard, irrigation maintains the SWC between 22–33% vol, whereas the Mediterranean maquis experiences drought periods (15% ≤ SWC ≤ 18% vol) during summer. Reduced physiological functions are observed during late spring and early fall (20% ≤ SWC ≤ 38% vol), but well-watered and optimum conditions (SWC > 38% vol) occur during the cold months.

Consistent with previous studies in semi-arid ecosystems (e.g. Huxman et al., 2004), at both sites, the variation of β shows that higher SWC enables more CO$_2$ uptake. GPP is more responsive to well-watered conditions than R$_{eco}$, as plants reach their optimum carbon uptake at high SWC levels, but in water stress conditions they use the carbon previously stored (Adams et al., 2009). At the Serdiana vineyard, the highest β value, 8.80 µmol m^{-2} s^{-1}, corresponds to when more irrigation occurred (23% ≤ SWC ≤ 33% vol), whereas at the Capo Caccia site, β is 13.1 µmol m^{-2} s^{-1} when the SWC was greater than 38% vol. The three months (January–March 2011) used to test the *general* model in the natural Mediterranean maquis site have well-watered conditions (SWC from 40.4% vol in March, to 43.5% vol in January).

A summary of the estimated β coefficients for the seven sites in Table 1 as a function of vegetation cover is shown in Fig. 3. The linear regression result, with the inclusion of the Helsinki most vegetated sector (summer weekends 2011 and 2012, 16.347 µmol m^{-2} s^{-1}) and the Sardinian sites at the highest SWC, improves the explanation (R^2 = 0.92).
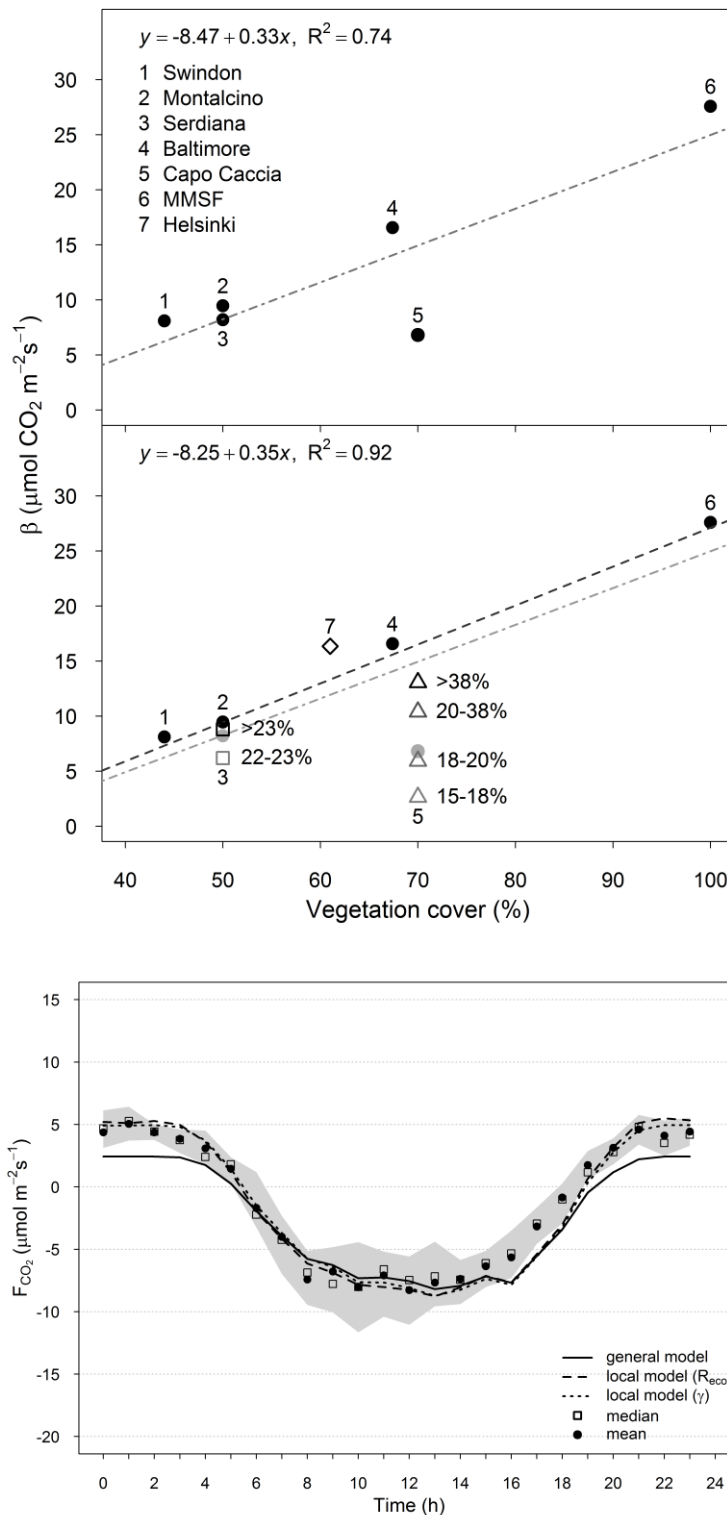
Fig. 3: *Variability of the plateau parameter (β, range between ecosystem respiration and maximum uptake of CO₂) as a function of vegetation cover. Top: linear regression analysis across the six sites in Table 2 (filled markers). Bottom: linear regression analysis across the six initial sites (with Serdiana vineyard (square) and Capo Caccia Mediterranean maquis (triangle), stratified in classes of soil water content (SWC), and considered only at 23% and >38% SWC, respectively) and the Helsinki most vegetated sector (diamond, summer weekends 2011–2012).*

4.2 Ecosystem respiration: constant intercept vs temperature driven equation

An estimate of the ecosystem respiration can be obtained with both R_{eco} being the intercept in the equation used to fit the light-response curves (γ, e.g. Eq. 2), or by a temperature driven equation (e.g. Eq. 4). A major difference between the *general* and *local* models is the introduction of R_{eco} (Eq. 4) into the non-rectangular hyperbola. To evaluate the impact of adding information to this equation, three simulations are undertaken (Fig. 4) to consider both R_{eco} and γ (not shown for the *local* model). Replacing R_{eco} (Eq. 4) into the NRH (Eq. 3) in the *local* model does not improve the diurnal mean simulation. The two model runs have similar metrics (RMSE = 0.34 μmol m⁻² s⁻¹, nRMSE = 0.02, R^2 = 1). The difference between the observed and modelled respiration using R_{eco} and γ is 5%, and 6%, respectively. Other temperature-driven equations (e.g. Lloyd and Taylor, 1994) may provide better performance, especially to reproduce short-term temporal scales (daily resolution). Evaluating using 30 minutes or hourly resolution data, a difference between R_{eco} and γ is evident with greater T_{air} variability across different days (not shown).

Fig. 4: *Observed (dots, shading IQR hourly means) mean CO₂ flux data at the Helsinki most vegetated sector (summer weekends 2010) and model results: general model (solid line, Eq. 3), local model (dashed line, Eq. 5 and Eq. 4), and local model using a constant intercept γ (dotted line, Eq. 5).*

The mean of all three simulations (Fig. 4), fall within the range of the measured standard deviations of the hourly means. The *general* model has lower values throughout the nocturnal period, possibly due to the assumptions and approximations made to create the empirical model using the data from six different sites (four without major anthropogenic emissions). Adding more sites to the analysis, as shown in Fig. 3 with the addition of Helsinki, would strengthen the *general* relations (Eq. 6) on which the empirical model is based.

5 Conclusions

In this study CO₂ eddy covariance fluxes for periods of maximum ecophysiological processes are investigated. Seven ecosystems, with different percentages of vegetation cover, are analysed to better understand the impact of vegetation on carbon emissions in the urban environment (e.g. to reduce net emissions), and to develop two different modelling approaches. Analysis of light-response curves from different sites highlights the similarities in CO₂ uptake between urban and non-urban ecosystems with respect to λ_V (independently of vegetation type), with $R^2 \geq 0.5$ (Eq. 6). This result agrees with previous EC fluxes studies across different neighbourhoods of the same (or nearby) city (Coutts et al., 2007; Bergeron and Strachan, 2011; Ramamurthy and Pardyjak, 2011; Nordbo et al., 2012; Ward et al., 2015) but widens the range to explore urban and non-urban ecosystems in the northern hemisphere.

The developed modelling approaches are based on the non-rectangular hyperbola, the vegetation cover fraction and common environmental variables to simulate the diurnal trend of vertical biogenic CO₂ fluxes. Evaluation of the *general* model with

independent data from the Capo Caccia Mediterranean maquis ecosystem and Helsinki suburban area show good agreement (explaining up to 98% of total variance). However, there is a systematic nocturnal underestimation. The best performance, has a nocturnal underestimation of 1.13 μmol m^{-2} s^{-1} (about 28%) for the suburban *general* case. This is probably related to the residual traffic and human respiration contribution to nocturnal CO_2 fluxes combined with the approximations made to use the generalised equations (Eq. 6).

The influence of soil water content on CO_2 fluxes is investigated for the Mediterranean sites, characterised by rainless periods and other summer environmental stress conditions. Improved performance metrics are obtained for the estimation of the generalised NRH plateau parameter (β) when considering well-watered conditions at the Sardinian sites and the most vegetated wind sector of Helsinki study area (R^2 = 92%). This finding, beyond highlighting the biogenic character of the model, demonstrates that the model can capture general trends across different ecosystems. This indicates it would be fruitful to add more sites (urban and non-urban) to strengthen the statistics and identify a range for the NRH coefficients as a function of vegetation cover, type and soil water content. Generalised parameters allow the estimation of the local biogenic contribution to CO_2 urban emissions when direct estimate of site-specific NRH coefficients are unavailable. However (unsurprisingly), performance metrics are better when using site-specific NRH coefficients. In this context, the *local* model developed and tested in Helsinki performs better for summer weekends within the vegetated wind sector (~5% underestimation in CO_2 nocturnal fluxes). Substituting the NRH intercept (γ) with a temperature driven equation (Eq. 4) to estimate R_{eco} does not improve the quality of long-term (month, season) simulations. Thus, a fixed value (i.e. γ) could be used to simplify the method.

Although both models simulate reasonably well in areas with large amounts of vegetation, we do not explicitly conclude which is best. Under present conditions, the *local* model is the most reliable approach, but the good performances of the *general* model make it a valid modelling option. As anthropogenic effects are minimized in this study, if local anthropogenic emissions were correctly described, the *local* model would presumably be better than the *general* model. Additionally, taking soil water availability into account in urban areas and using the temperature based R_{eco} is expected to be beneficial.

6 Acknowledgements

References

Adams, H.D., Guardiola–Claramonte, M., Barron–Gafford, G.A., Villegas, J.C., Breshears, D.D., Zou, C.B., Troch, P.A., and Huxman, T.E. (2009). Temperature sensitivity of drought-induced tree mortality portends increased regional die-off under global-change-type drought. Proceedings of the National Academy of Sciences, 106(17):7063–7066. doi:10.1073/pnas.0901438106.

Aubinet, M., Grelle, A., Ibrom, A., Rannik, Ü., Moncrieff, J., Foken, T., Kowalski, A.S., Martin, P.H., Berbigier, P., Bernhofer, C., Clement, R., Elbers, J., Granier, A., Grünwald, T., Morgenstern, K., Pilegaard, K., Rebmann, C., Snijders, W., Valentini, R., Vesala, T. (1999). Estimates of the annual net carbon and water exchange of forests: the EUROFLUX methodology. Advances in Ecological Research, 30:113–175. doi: 10.1016/S0065-2504(08)60018-5.

Baldocchi, D. (1997). Flux footprints within and over forest canopies. Boundary-Layer Meteorology, 85(2):273–292. doi: 10.1023/A:1000472717236.

Bergeron, O., and Strachan, I.B. (2011). CO_2 sources and sinks in urban and suburban areas of a northern mid-latitude city. Atmospheric Environment, 45(8):1564–1573. doi:10.1016/j.atmosenv.2010.12.043.

Bjorkegren, A., and Grimmond, C.S.B. (2016) Net Carbon Dioxide emissions from central London. Urban Climate (in press). UCLIM-D-16-00071R1.

Boote, K.J., and Loomis, R.S. (1991). The prediction of canopy assimilation. In: Modeling Crop Photosynthesis–from Biochemistry to Canopy. Boote, K.J., and Loomis, R.S. (eds.). Crop Science Society of America, Madison, WI. CCSA Special Publication, 19:109–137.

Christen, A., Coops, N., Crawford, B., Kellett, R., Liss, K., Olchovski, I., Tooke, T., Van Der Laan, M., and Voogt, J. (2011). Validation of modeled carbon-dioxide emissions from an urban neighborhood with direct eddy covariance measurements. Atmospheric Environment, 45(33):6057–6069. doi:10.1016/j.atmosenv.2011.07.040.

Coutts, A.M., Beringer, J., and Tapper, N.J. (2007). Characteristics influencing the variability of urban CO_2 fluxes in Melbourne, Australia. Atmospheric Environment, 41(1):51–62. doi:10.1016/j.atmosenv.2006.08.030.

Crawford, B., Grimmond, C.S.B., and Christen, A. (2011). Five years of carbon dioxide fluxes measurements in a highly vegetated suburban area. Atmospheric Environment, 45(4):896–905. doi:10.1016/j.atmosenv.2010.11.017.

Crawford, B., and Christen, A. (2015). Spatial source attribution of measured urban eddy covariance CO_2 fluxes. Theoretical and Applied Climatology, 119(3):733–755. doi:10.1007/s00704-014-1124-0.

Decina, S.M., Hutyra, L.R., Gately, C.K., Getson, J.M., Reinmann, A.B., Gianotti, A.G.S., and Templer, P.H. (2016). Soil respiration contributes substantially to urban carbon fluxes in the greater Boston area. Environmental Pollution, 212:433–439. doi:10.1016/j.envpol.2016.01.012.

Gilmanov, T.G., Verma, S.B., Sims, P.L., Meyers, T.P., Bradford, J.A., Burba, G.G., and Suyker, A.E. (2003). Gross primary production and light-response parameters of four Southern Plains ecosystems estimated using long-term CO_2-flux tower measurements. Global Biogeochemical Cycles, 17(2). doi:10.1029/2002GB002023.

Grimmond, C.S.B., and Christen, A. (2012). Flux measurements in urban ecosystems. FluxLetter, 5(1):1–8.

Helfter, C., Famulari, D., Phillips, G.J., Barlow, J.F., Wood, C.R., Grimmond, C.S.B., and Nemitz, E. (2011). Controls of carbon dioxide concentrations and fluxes above central London. Atmospheric Chemistry and Physics, 11(5), 1913–1928. doi:10.5194/acp-11-1913-2011.

Huxman, T.E., Snyder, K.A., Tissue, D., Leffler, A.J., Ogle, K., Pockman, W.T., Sandquist, D.R., Potts, D.L., and Schwinning, S. (2004). Precipitation pulses and carbon fluxes in semiarid and arid ecosystems. Oecologia, 141(2):254–268. doi:10.1007/s00442-004-1682-4.

IEA (2008). World Energy Outlook 2008. OECD Publishing, Paris. 10.1787/weo-2008-en.

Järvi, L., Mammarella, I., Eugster, W., Ibrom, A., Siivola, E., Dellwik, E., Keronen, P., Burba, G., and Vesala, T. (2009). Comparison of net CO_2 fluxes measured with open- and closed-path infrared gas analyzers in an urban complex environment. Boreal Environment Research, 14:499–514.

Järvi, L., Grimmond, C.S.B., and Christen, A. (2011). The Surface Urban Energy and Water Balance Scheme (SUEWS): Evaluation in Los Angeles and Vancouver. Journal of Hydrology, 411(3), 219-237. doi:10.1016/j.jhydrol.2011.10.001.

Järvi, L., Nordbo, A., Junninen, H., Riikonen, A., Moilanen, J., Nikinmaa, E., and Vesala, T. (2012). Seasonal and annual variation of carbon dioxide surface fluxes in Helsinki, Finland, in 2006–2010. Atmospheric Chemistry and Physics, 12(18):8475–8489. doi:10.5194/acp-12-8475-2012.

Järvi, L., Grimmond, C.S.B., Taka, M., Nordbo, A., Setälä, H., and Strachan, I.B. (2014). Development of the Surface Urban Energy and Water Balance Scheme (SUEWS) for cold climate cities. Geoscientific Model Development, 7(4):1691–1711. doi:10.5194/gmd-7-1691-2014.

Jo, H.K., and McPherson, E.G. (1995). Carbon storage and flux in urban residential greenspace. Journal of Environmental Management, 45(2):109–133. doi:10.1006/jema.1995.0062.

Lasslop, G., Reichstein, M., Papale, D., Richardson, A.D., Arneth, A., Barr, A., Stoy, P., and Wohlfahrt, G. (2010). Separation of net ecosystem exchange into assimilation and respiration using a light-response curve approach: critical issues and global evaluation. Global Change Biology, 16(1):187–208. doi:10.1111/j.1365-2486.2009.02041.x.

Le Quéré, C., Moriarty, R., Andrew, R.M., Canadell, J.G., Sitch, S., Korsbakken, J.I., Friedlingstein, P., Peters, G.P., Andres, R.J., Boden, T.A., Houghton, R.A., House, J.I., Keeling, R.F., Tans, P., Arneth, A., Bakker, D.C.E., Barbero, L., Bopp, L., Chang, J., Chevallier, F., Chini, L.P., Ciais, P., Fader, M., Feely, R.A., Gkritzalis, T., Harris, I., Hauck, J., Ilyina, T., Jain, A.K., Kato, E., Kitidis, V., Klein Goldewijk, K., Koven, C., Landschützer, P., Lauvset, S.K., Lefèvre, N., Lenton, A., Lima, I.D., Metzl, N., Millero, F., Munro, D.R., Murata, A., Nabel, J.E.M.S., Nakaoka, S., Nojiri, Y., O'Brien, K., Olsen, A., Ono, T., Pérez, F.F., Pfeil, B., Pierrot, D., Poulter, B., Rehder, G., Rödenbeck, C., Saito, S., Schuster, U., Schwinger, J., Séférian, R., Steinhoff, T., Stocker, B.D., Sutton, A.J., Takahashi, T., Tilbrook, B., van der Laan-Luijkx, I.T., van der Werf, G.R., van Heuven, S., Vandemark, D., Viovy, N., Wiltshire, A., Zaehle, S., and Zeng, N. (2015). Global Carbon Budget 2015, Earth System Science Data, 7, 349-396, doi:10.5194/essd-7-349-2015, 2015.

Lloyd, J., and Taylor, J. (1994). On the temperature dependence of soil respiration. Functional ecology, 8:315–323. doi:10.2307/2389824.

Marcotullio, P.J., Sarzynski, A., Albrecht, J., Schulz, N., and Garcia, J. (2013). The geography of global urban greenhouse gas emissions: an exploratory analysis. Climatic Change, 121(4): 621–634. doi:10.1007/s10584-013-0977-z.

Marcotullio, P.J. (2016). Urbanization, energy use and greenhouse gas emissions. In: The Routledge Handbook of Urbanization and Global Environmental Change. Seto, K.C., Solecki, W.D., and Griffith, C.A. (eds.). London: Routledge. 106–124.

Marras, S. (2008). Evaluation of the Advanced Canopy-Atmosphere-Soil Algorithm (ACASA) model performance using micrometeorological techniques. PhD thesis in Agrometeorology and Ecophysiology of Agricultural and Forest Ecosystems, University of Sassari.

Marras, S., Pyles, R.D., Sirca, C., Paw U, K.T., Snyder, R.L., Duce, P., and Spano, D. (2011). Evaluation of the Advanced Canopy-Atmosphere-Soil Algorithm (ACASA) model performance over Mediterranean maquis ecosystem. Agricultural and Forest Meteorology, 151(6):730–745. doi:10.1016/j.agrformet.2011.02.004.

Marras, S., Masia, S., Duce, P., Spano, D., and Sirca, C. (2015). Carbon footprint assessment on a mature vineyard. Agricultural and Forest Meteorology, 214:350–356. doi:10.1016/j.agrformet.2015.08.270.

Marshall, B., and Biscoe, P.V. (1980). A model for C_3 leaves describing the dependence of net photosynthesis on irradiance. Journal of Experimental Botany, 31(120):29–39. doi:10.1093/jxb/31.1.29.

Matese, A., Gioli, B., Vaccari, F., Zaldei, A., and Miglietta, F. (2009). Carbon dioxide emissions of the city center of Firenze, Italy: measurement, evaluation, and source partitioning. Journal of Applied Meteorology and Climatology, 48(9):1940–1947. doi:10.1175/2009JAMC1945.1.

Moriwaki, R., and Kanda, M. (2004). Seasonal and diurnal fluxes of radiation, heat, water vapor, and carbon dioxide over a suburban area. Journal of Applied Meteorology, 43(11):1700–1710. doi:10.1175/JAM2153.1.

Nemitz, E., Hargreaves, K.J., McDonald, A.G., Dorsey, J.R., and Fowler, D. (2002). Micrometeorological measurements of the urban heat budget and CO_2 emissions on a city scale. Environmental Science & Technology, 36(14):3139–3146. doi:10.1021/es010277e.

Nordbo, A., Järvi, L., Haapanala, S., Wood, C.R., and Vesala, T. (2012). Fraction of natural area as main predictor of net CO_2 emissions from cities. Geophysical Research Letters, 39(20). doi:10.1029/2012GL053087.

Nowak, D.J., Crane, D.E., Stevens, J.C., Hoehn, R.E., Walton, J.T., and Bond, J. (2008). A ground-based method of assessing urban forest structure and ecosystem services. Arboriculture & Urban Forestry, 34(6):347–358.

Ögren, E. (1993). Convexity of the photosynthetic light-response curve in relation to intensity and direction of light during growth. Plant Physiology, 101(3):1013–1019.

Papale, D., Reichstein, M., Canfora, E., Aubinet, M., Bernhofer, C., Longdoz, B., Kutsch, W., Rambal, S., Valentini, R., Vesala, T., and Yakir, D. (2006). Towards a standardized processing of Net Ecosystem Exchange measured with eddy covariance technique: algorithms and uncertainty estimation. Biogeosciences, 3(4):571–583. doi:10.5194/bg-3-571-2006, 2006.

Park, M.S., Joo, S.J., and Lee, C.S. (2013). Effects of an urban park and residential area on the atmospheric CO_2 concentration and flux in Seoul, Korea. Advances in Atmospheric Sciences, 30(2):503–514. doi:10.1007/s00376-012-2079-7.

Peters, E.B., and McFadden, J.P. (2012). Continuous measurements of net CO_2 exchange by vegetation and soils in a suburban landscape. Journal of Geophysical Research: Biogeosciences, 117(G3):1–16. doi: 10.1029/2011JG001933.

Rabinowitch, E.I. (1951). Photosynthesis and related processes, Vol 2(1). Interscience Publishers, New York, NY.

Ramamurthy, P., and Pardyjak, E.R. (2011). Toward understanding the behavior of carbon dioxide and surface energy fluxes in the urbanized semiarid Salt Lake Valley, Utah, USA. Atmospheric Environment, 45(1):73–84. doi:10.1016/j.atmosenv.2010.09.049.

Rosenzweig, C., Solecki, W., Hammer, S.A., and Mehrotra, S. (2010). Cities lead the way in climate-change action. Nature, 467(7318):909–911. doi:10.1038/467909a.

Ruimy, A., Jarvis, P., Baldocchi, D., and Saugier, B. (1995). CO_2 fluxes over plant canopies and solar radiation: a review. Advances in Ecological Research, 26:1–68. doi:10.1016/S0065-2504(08)60063-X.

Satterthwaite, D. (2008). Cities' contribution to global warming: notes on the allocation of greenhouse gas emissions. Environment and urbanization, 20(2):539–549. doi:10.1177/0956247808096127.

Schmid, H.P., Grimmond, C.S.B., Cropley, F., Offerle, B., and Su, H.–B. (2000). Measurements of CO_2 and energy fluxes over a mixed hardwood forest in the mid-western United States. Agricultural and Forest Meteorology, 103(4):357–374. doi:10.1016/S0168-1923(00)00140-4.

Soegaard, H., and Møller-Jensen, L. (2003). Towards a spatial CO_2 budget of a metropolitan region based on textural image classification and flux measurements. Remote Sensing of Environment, 87(2):283–294. doi:10.1016/S0034-4257(03)00185-8.

Bellucco V, S Marras, CSB Grimmond, L Järvi, C Sirca, D Spano (2017) Modelling the biogenic CO_2 exchange in urban and non-urban ecosystems through the assessment of light-response curve parameters *Agricultural and Forest Meteorology* http://dx.doi.org/10.1016/j.agrformet.2016.12.011

IPCC, 2013: Summary for Policymakers. In: Climate Change 2013: The Physical Science Basis. Contribution of Working Group I to the Fifth Assessment Report of the Intergovernmental Panel on Climate Change. Stocker, T.F., Qin, D., Plattner, G.–K., Tignor, M., Allen, S.K., Boschung, J., Nauels, A., Xia, Y., Bex, V., and Midgley, P.M. (eds.). Cambridge University Press, Cambridge, United Kingdom and New York, NY, USA.

Stoy, P.C., Katul, G.G., Siqueira, M., Juang, J.–Y., Novick, K.A., Uebelherr, J.M., and Oren, R. (2006). An evaluation of models for partitioning eddy covariance-measured net ecosystem exchange into photosynthesis and respiration. Agricultural and Forest Meteorology, 141(1):2–18. doi:10.1016/j.agrformet.2006.09.001.

Tsubo, M., and Walker, S. (2005). Relationships between photosynthetically active radiation and clearness index at Bloemfontein, South Africa. Theoretical and Applied Climatology, 80(1):17–25. doi:10.1007/s00704-004-0080-5.

United Nations (UN), Department of Economic and Social Affairs, Population Division (2014). World Urbanization Prospects: The 2014 Revision, Highlights (ST/ESA/SER.A/352). New York. ISBN 978-92-1-151517-6.

Velasco, E., Pressley, S., Grivicke, R., Allwine, E., Coons, T., Foster, W., Jobson, B., Westberg, H., Ramos, R., Hernández, F., Molina, L.T., and Lamb, B. (2009). Eddy covariance flux measurements of pollutant gases in urban Mexico City. Atmospheric Chemistry and Physics, 9(19):7325–7342. doi:10.5194/acp-9-7325-2009.

Velasco, E., and Roth, M. (2010). Cities as net sources of CO_2: Review of atmospheric CO_2 exchange in urban environments measured by eddy covariance technique. Geography Compass, 4(9):1238–1259. doi:10.1111/j.1749-8198.2010.00384.x.

Velasco, E., Roth, M., Tan, S., Quak, M., Nabarro, S., and Norford, L. (2013). The role of vegetation in the CO_2 flux from a tropical urban neighbourhood. Atmospheric Chemistry and Physics, 13(20):10185–10202. doi:10.5194/acp-13-10185-2013.

Velasco, E., Roth, M., Norford, L., and Molina, L.T. (2016). Does urban vegetation enhance carbon sequestration? Landscape and Urban Planning, 148:99–107. doi: 10.1016/j.landurbplan.2015.12.003.

Vesala, T., Järvi, L., Launiainen, S., Sogachev, A., Rannik, Ü., Mammarella, I., Siivola, E., Keronen, P., Rinne, J., Riikonen, A., and Nikinmaa, E. (2008). Surface–atmosphere interactions over complex urban terrain in Helsinki, Finland. Tellus B, 60(2):188–199. doi:10.1111/j.1600-0889.2007.00312.x.

Ward, H.C., Evans, J.G., and Grimmond, C.S.B. (2013). Multi-season eddy covariance observations of energy, water and carbon fluxes over a suburban area in Swindon, UK. Atmospheric Chemistry and Physics, 13(9):4645–4666. doi:10.5194/acp-13-4645-2013.

Ward, H.C., Kotthaus, S., Grimmond, C.S.B., Bjorkegren, A., Wilkinson, M., Morrison, W.T.J., Evans, J.G., Morison, J.I.L., and Iamarino, M. (2015). Effects of urban density on carbon dioxide exchanges: Observations of dense urban, suburban and woodland areas of southern England. Environmental Pollution, 198:186–200. doi:10.1016/j.envpol.2014.12.031.

Webb, E.K., Pearman, G.I., and Leuning, R. (1980). Correction of flux measurements for density effects due to heat and water vapour transfer. Quarterly Journal of the Royal Meteorological Society, 106(447):85–100. doi: 10.1002/qj.49710644707.

Weissert, L.F., Salmond, J.A., and Schwendenmann, L. (2014). A review of the current progress in quantifying the potential of urban forests to mitigate urban CO_2 emissions. Urban Climate, 8:100–125. doi: 10.1016/j.uclim.2014.01.002.

World Meteorological Organization, World Data Centre for Greenhouse Gases (2015). WMO Greenhouse Gas Bulletin. The State of Greenhouse Gases in the Atmosphere Based on Global Observations Through 2014. No.11. ISSN 2078-0796.